

# Investigations of the Oxy-Fuel Coal Char Gasification Reactions Kinetics in the Isothermal Drop-Tube Furnace

J. Hercog\*, B. Świątkowski

Institute of Power Engineering, Augustówka 36, 02-981 Warsaw, Poland

## Abstract

The influence of the individual gasification reactions, with CO<sub>2</sub> and H<sub>2</sub>O, occurring on the coal char particle surface during oxy-fuel combustion was addressed in this paper. The experimental results were used to derive the individual reaction kinetic parameters using ash tracer method and fitting data algorithm. Data analysis was supported by the CFD modelling providing thermal histories of the particles, i.e. temperatures and residence times. The overall char combustion model was modified in order to include the influence of the individual gasification reactions on the particle surface reaction rate and was implemented in the commercial CFD code. Numerical simulations of the oxy-fuel char gasification in drop-tube have been carried out, and results are in reasonable consistency with the experimental data.

## Nomenclature

$\Delta H$	heat of reaction, kJ/kmol,
$\dot{n}''$	molar flux, kmol/(s·m <sup>2</sup> ),
X <sub>C</sub>	char conversion (char burnout),
$\rho$	density, kg/m <sup>3</sup> ,
$A$	preexponential factor, (different units),
$C$	molar concentration, kmol/m <sup>3</sup> ,
$c_p$	particle specific heat capacity, J/(kg·K),
$D$	effective diffusion coefficient, m <sup>2</sup> /s,
$d_p$	particle diameter, m,
$E$	activation energy, J/kmol,
$f$	mass fraction,
$k_c$	reaction rate coefficient, (different units),
$k_d$	mass transfer coefficient, m/s,
$M$	molecular mass, kg/kmol,
$m$	mass, kg,
$p$	pressure, Pa,
$r$	radius, m or reaction rate, kg/s,
$T$	temperature, K,
$t$	time, s,
$V$	volume, m <sup>3</sup> ,
$y$	mole fraction,
<b>Subscripts</b>	
$\infty$	free stream,
$C$	carbon,
$a$	ash,
$f$	fluid,
$g$	gas species index,
$i$	reaction index,
$p$	particle,
$s$	surface,
0	initial state.

## 1. Introduction

One of the most promising measures of the CO<sub>2</sub> emission abatement from coal fired power plants is oxy-fuel combustion, due to its lowest energy penalty associated with the investment and operational costs [1]. The main feature of the oxy-fuel technology is an elimination of air from the combustion system and its replacement with the mixture of recycled flue gases (mainly CO<sub>2</sub> and H<sub>2</sub>O) and O<sub>2</sub>. In consequence, the flue gas mainly comprises of CO<sub>2</sub>, which significantly increases its removal efficiency. But this action can alter the combustion process due to different physical and chemical properties of diluents such as CO<sub>2</sub> and H<sub>2</sub>O in respect to N<sub>2</sub> [2]. Flame and particle temperatures, heat transfer, emissions and burnout can be changed [3, 4], which can be caused by different gas properties and/or combustion mechanism.

Naredi and Pisupati [5] observed that the char burnouts are lower during oxy-fuel combustion compared to in air for 2 ranks of bituminous coal, most likely due to lower particle temperature, however the difference becomes smaller at higher temperatures, which can be explained by an increase of the gasification reaction with CO<sub>2</sub>.

Brix *et al.* [6] have conducted char combustion experiments in EFR and found no evidence of the gasification reaction with CO<sub>2</sub> in a range of operating conditions, but the modelling of the process suggests that the gasification may occur where there are low concentrations of O<sub>2</sub>, high temperatures and bigger particles.

However, Gonzalo-Tirado *et al.* [7] stated in their work that gasification reactions can contribute to the overall char consumption rate and compensate for the changes in the gaseous atmosphere at the low oxygen concentrations.

In this study a series of laboratory experiments have been conducted in isothermal drop-tube to assess the

\*Corresponding author.

Email address: jaroslaw.hercog@ien.com.pl (J. Hercog)

char gasification rates with  $\text{CO}_2$  and  $\text{H}_2\text{O}$  and include their influence on the total char consumption in commercial CFD code.

## 2. Experimental setup

### 2.1. Char combustion facility

The experiments were conducted in the facility, showed in Fig. 1, which main element is an electrically heated, silicon carbide drop-tube with a 38.5 mm inner diameter and 6-meter length. The desired reaction atmosphere composition is formed using mass flow controllers. Pulverized solid fuel is dosed using the precise screw feeder, and pneumatically transported by the cold, primary gas to the reactor through the one of the twelve, sloped ports installed along the reactor height. The particle residence time was varied by changing the position of the feeding probe while the collection point remained stationary.

### 2.2. Char properties

Bituminous coal, originating from Poland, was selected for experiments. Before the tests, raw fuel was dried, milled and sieved in order to obtain the desired particle size in a range of 63–80  $\mu\text{m}$ . Then the pulverized fuel was devolatilised at 1300 °C at high heating rate of  $10^4$  K/s in pure nitrogen. The residence time for devolatilization test was set up to 250 ms ensuring complete devolatilisation. The char and parent fuel properties, on analytic basis, are collected in Tab. 1. Char particle size distribution is presented in Fig. 2.

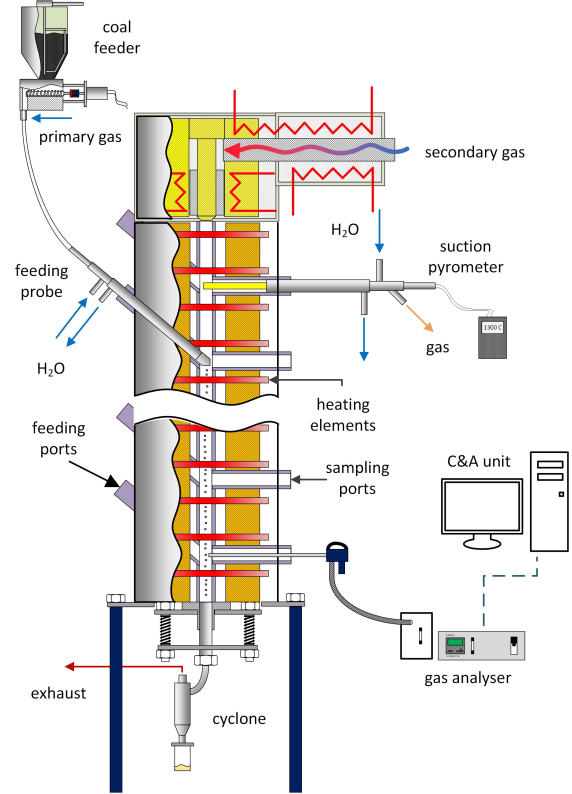


Figure 1: Char combustion facility

Table 1: Parent fuel and char properties

quantity	parent coal	char
M, %wt.	5.6	2.6
A, %wt.	10.9	11.5
VM, %wt.	32.5	1.4
C, %wt.	63.90	74.60
H, %wt.	4.08	0.27
N, %wt.	1.11	1.29
S, %wt.	1.25	1.02
$O_{diff}$ , %wt.	13.25	0.18
HCV, kJ/kg	25097	26614
LCV, kJ/kg	26492	24071
$\bar{d}$ , $\mu\text{m}$	-	71

### 2.3. Methodology

Experiments were carried out in the following conditions:

- reaction temperatures: 900, 1050 and 1200 °C,
- for gasification with  $\text{CO}_2$  :  $\text{CO}_2$  mole fraction in  $\text{N}_2$ : 50%, 70%, 90%,

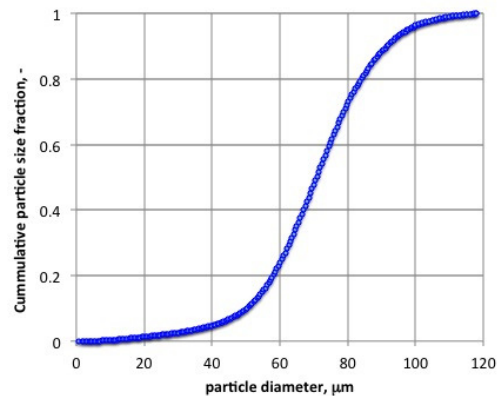


Figure 2: Cumulative char particle size distribution

- for gasification with H<sub>2</sub>O : H<sub>2</sub>O mole fraction in N<sub>2</sub>: 20%, 30%, 40%,
- residence time varying from 0.1 to 1.5 s.

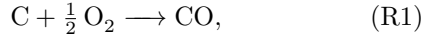
Conversion levels (char burnout) were calculated by the following equation

$$X_C = \frac{f_a - f_{a,0}}{f_a(1 - f_{a,0})} \quad (1)$$

derived on the basis of the ash tracer method [8].

### 3. Char combustion model

In this study the single-film model [9, 10] has been adopted, since is acceptable model for particle sizes up to 100  $\mu\text{m}$  [11] and is widely used to describe char combustion, especially in CFD. When pulverized char particles are burnt in oxy-fuel conditions, the combustion mechanism, besides oxidation, additionally should take into consideration the gasification with CO<sub>2</sub> and H<sub>2</sub>O. The combustion mechanism of char carbon is composed of three surface reactions and defined as follows:



The total rate of char carbon consumption,  $r_C$ , is defined as follows

$$r_C = \sum_{i=1}^{i=3} r_{C,i} \quad (2)$$

where  $i$  numbers the  $i$ -th surface reaction, and

$$r_{C,i} = A_p M_C \psi_i |\dot{\mathbf{n}}_g''| \quad (3)$$

in which  $g \in \{\text{O}_2, \text{CO}_2, \text{H}_2\text{O}\}$  for  $i \in \{1, 2, 3\}$  respectively,  $A_p = \pi d_p^2$  is the reaction area expressed as the external particle surface,  $\psi_1 = 2 \text{ mol-C/mol-O}_2$ ,  $\psi_2 = 1 \text{ mol-C/mol-CO}_2$  and  $\psi_3 = 1 \text{ mol-C/mol-H}_2\text{O}$ .

The molar flux of the  $g$ -th gas reagent,  $\dot{\mathbf{n}}_g''$ , results from the balance of rates between gas diffusion and the surface reaction, i.e.

$$|\dot{\mathbf{n}}_g''| = k_d C \ln \left( \frac{y_{g,\infty} + 1}{y_{g,s} + 1} \right) = k_{c,i} C_{g,s}^{m_i} \quad (4)$$

where

$$C = \frac{p}{RT_s} \quad (5)$$

is the total molar concentration,

$$k_d = \frac{D}{r_p} \quad (6)$$

is the mass transfer coefficient,

$$k_{c,i} = A_i T^{\beta_i} e^{-E_i/(RT_s)} \quad (7)$$

is the rate coefficient of the  $i$ -th surface reaction expressed in the form of the modified Arrhenius equation.

In the current study, it is assumed that the reactions (R1), (R2) and (R3) are independent of each other allowing to write the molar flux of the  $g$ -th gas reagent as Eq.(4) which mathematically presents the single-film model for char combustion in the current approach.

The effective diffusion coefficient,  $D$ , expressed as [9, 12]

$$D(T) = D_0 \left( \frac{T_{f,\infty} + T_p(t)}{2T_0} \right)^{1.75}, \quad (8)$$

has got different values for air and oxy-fuel combustion. Namely, at air combustion, just the oxidation reaction (R1) is considered to be important in the combustion mechanism so that  $D_0^{air} = D_{\text{O}_2-\text{N}_2} = 0.181 \text{ cm}^2/\text{s}$  at  $T_0 = 273 \text{ K}$  [13]. At oxy-fuel combustion, also reactions (R2) and (R3) are expected to be active but the in the present conditions they are completely kinetically controlled [14], so that

$$r_{C,2} = A_p M_C \psi_2 k_{c,2} C_{\text{CO}_2,\infty} \quad (9)$$

$$r_{C,3} = A_p M_C \psi_3 k_{c,3} C_{\text{H}_2\text{O},\infty} \quad (10)$$

are applied in the current model.

Finally, the governing equations of the char combustion model can be presented. It is assumed that the char particle is treated as a discrete Lagrange particle. It was assumed that the particle volume,  $V_p = \frac{\pi}{6} d_p^3$ , is constant during combustion, so that the mass conservation law of the char particle is expressed in the following form:

$$V_p \frac{d\rho_p}{dt} = -r_C(t), \quad \rho_p(0) = \rho_{p,0} \quad (11)$$

and the char particle mass is then defined as

$$m_p(t) = m_a + m_C(t) \quad (12)$$

in which

$$m_a = f_{a,0} \rho_{p,0} V_p \quad (13)$$

is constant mass of ash contained in the char particle. The char particle temperature,  $T_p(t)$ , is defined by the conservation law of particle energy as follows [15]:

$$m_p(t) c_p \frac{dT_p(t)}{dt} = h A_p (T_{f,\infty} - T_p(t)) + A_p \varepsilon_p \sigma (T_{f,\infty}^4 - T_p^4(t)) + \sum_{i=1}^{i=3} r_{C,i}(t) \Delta H_i \quad (14)$$

with the initial condition

$$T_p(t=0) = T_{p,0}, \quad (15)$$

where the heat transfer coefficient  $h$  is defined as

$$h = \frac{k_{f,\infty}}{d_p} \text{Nu} \quad (16)$$

in which  $\text{Nu} = 2 + 0.6 \text{Re}_p^{1/2} \text{Pr}^{1/3}$  is the Nusselt number.

#### 4. Results and discussion

A set of two ordinary differential equations have been determined by the generalized reduced gradient method [16] for which the fourth-order Runge-Kutta method was used to solve the system and thus determine the values of  $X_C^{num}$ . More details of the coupling of the Ansys Fluent and Matlab and determining of the kinetic parameters are given elsewhere [17]. Values of the optimal kinetic parameters determined in Matlab are presented in Tab. 2. Fig. 3 shows evo-

Table 2: Optimal values of the kinetic parameters

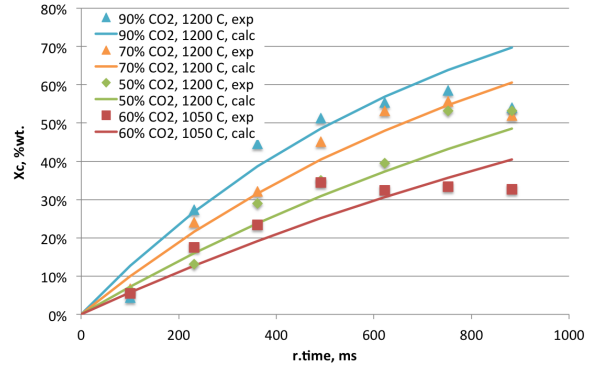
reaction	$A$	$E$
	kg/m <sup>2</sup> sPa	kJ/mol
gasification with CO <sub>2</sub>	$3.867 \times 10^{-6}$	46.3
gasification with H <sub>2</sub> O	$2.140 \times 10^{-1}$	179.5

lution of char consumption for examined coal char gasified with CO<sub>2</sub> and H<sub>2</sub>O. The gasification at low temperature (900 °C) and low mole concentration of H<sub>2</sub>O (20, 30 %<sub>mol.</sub>) was negligible (results not shown here). In present study the gasification reactions begin at higher temperatures ( $\geq 1050$  °C) and higher concentrations of H<sub>2</sub>O ( $\geq 40$  %<sub>mol.</sub>). It can also be noted that, in current experimental conditions, the gasification reaction can be responsible up to 60 and 50 %<sub>wt.</sub> of the char mass loss in case of gasification with CO<sub>2</sub> and H<sub>2</sub>O respectively. Even at reasonably low temperature (1050 °C) the gasification with CO<sub>2</sub> is not negligible, reaching 30%<sub>wt.</sub> after 500 ms.

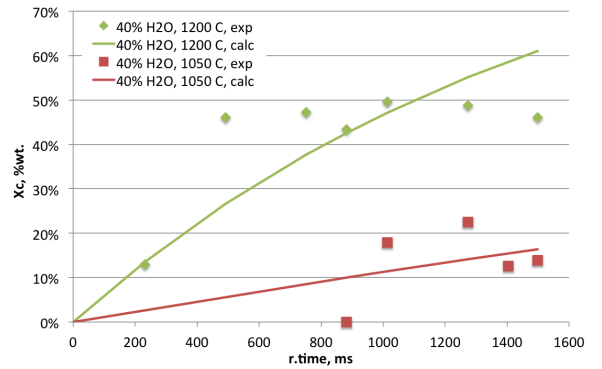
When the two reactions are compared it can be observed that gasification with H<sub>2</sub>O begins later than with CO<sub>2</sub>, exhibiting higher activation energy, but when the temperature is high enough (1200 °C) then the gasification rate with H<sub>2</sub>O is even higher than with CO<sub>2</sub> (see Fig. 4).

#### 5. Conclusions

Laboratory experiments of the coal char gasification with CO<sub>2</sub> and H<sub>2</sub>O, conducted in conditions comparable to pulverised fuel boilers, have shown that, at no presence of the O<sub>2</sub>, the char consumption due to gasification can be up to 60 %<sub>wt.</sub>, showing that at low oxygen concentrations, the gasification reactions may compensate for lower temperatures in oxy-fuel combustion conditions. On the other hand, it is necessary to include those reactions in combustion modelling, as they may influence the



(a) Gasification with CO<sub>2</sub>



(b) Gasification with H<sub>2</sub>O

Figure 3: Coal char gasification with CO<sub>2</sub> and H<sub>2</sub>O

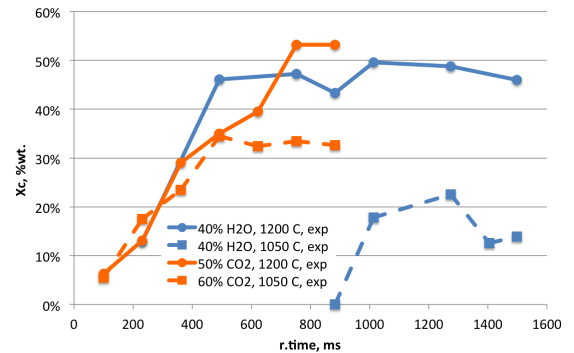


Figure 4: Comparison of the char gasification with CO<sub>2</sub> and H<sub>2</sub>O in selected conditions

overall combustion rate. Although the mathematical modelling, using combustion model presented in this study, showed reasonably good agreement with the experimental data, it seems that mutual effect of the surface reactions should be also addressed as the total reaction rate isn't most likely the simple sum of the three reactions.

#### Acknowledgments

The authors acknowledge financial assistance from the National Centre for Research and Development, within the confines of Research and Development

Strategic Program "Advanced Technologies for Energy Generation" project no. 2 "Oxy-combustion technology for PC and FBC boilers with CO<sub>2</sub> capture". Agreement no. SP/E/2/66420/10.

## References

- [1] K. E. Jenni, E. D. Baker, G. F. Nemet, *International Journal of Greenhouse Gas Control* 12 (2013) 136–145.
- [2] L. Chen, S. Z. Yong, A. F. Ghoniem, *Progress in Energy and Combustion Science* 38 (2012) 156–214.
- [3] M. B. Toftegaard, J. Brix, P. A. Jensen, P. Glarborg, A. D. Jensen, *Progress in Energy and Combustion Science* 36 (2010) 581–625.
- [4] B. Buhre, L. Elliott, C. Sheng, R. Gupta, T. Wall, *Progress in Energy and Combustion Science* 31 (2005) 283–307.
- [5] P. Naredi, S. Pisupati, *Energy & Fuels* 25 (2011) 2452–2459.
- [6] J. Brix, P. A. Jensen, A. D. Jensen, *Fuel* 90 (2011) 2224 – 2239.
- [7] C. Gonzalo-Tirado, S. Jiménez, J. Ballester, *Combustion and Flame* 159 (2012) 385 – 395.
- [8] S. Badzioch, P. G. W. Hawksley, *Ind. Eng. Chem. Process Des. Develop.*, 9 (1970) 521–530.
- [9] M. A. Field, *Combustion of pulverised coal*, Leatherhead (Sy.), B.C.U.R.A., 1967.
- [10] F. E. Fendell, *Combustion Science and Technology* 1 (1969) 13–24.
- [11] R. E. Mitchell, *Combustion Science and Technology* 53 (1987) 165–186.
- [12] M. M. Baum, P. J. Street, *Combustion Science and Technology* 3 (1971) 231–243.
- [13] D. W. Green, R. H. Perry, *Perry's Chemical Engineer's Handbook*, McGraw-Hill, 2008.
- [14] J. Hercog, R. Lewtak, 39rd International Technical Conference on Coal Utilization and Fuel Systems, Clearwater, FL, USA (2014).
- [15] R. Lewtak, A. Milewska, *Fuel* 113 (2013) 844 – 853.
- [16] L. S. Lasdon, A. D. Waren, A. Jain, M. Ratner, *ACM Trans. Math. Softw.* 4 (1978) 34–50.
- [17] A. Milewska, J. Hercog, 39rd International Technical Conference on Coal Utilization and Fuel Systems, Clearwater, FL, USA (2014).